

# Ordered Organelle Degradation during Starvation-induced Autophagy<sup>\*</sup>

Anders Riis Kristensen<sup>‡§</sup>, Søren Schandorff<sup>‡</sup>, Maria Høyer-Hansen<sup>¶</sup>,  
Maria Overbeck Nielsen<sup>‡</sup>, Marja Jäättelä<sup>¶</sup>, Jörn Dengjel<sup>||\*\*</sup>, and Jens S. Andersen<sup>‡||‡‡</sup>

**Upon starvation cells undergo autophagy, a cellular degradation pathway important in the turnover of whole organelles and long lived proteins. Starvation-induced protein degradation has been regarded as an unspecific bulk degradation process. We studied global protein dynamics during amino acid starvation-induced autophagy by quantitative mass spectrometry and were able to record nearly 1500 protein profiles during 36 h of starvation. Cluster analysis of the recorded protein profiles revealed that cytosolic proteins were degraded rapidly, whereas proteins annotated to various complexes and organelles were degraded later at different time periods. Inhibition of protein degradation pathways identified the lysosomal/autophagosomal system as the main degradative route. Thus, starvation induces degradation via autophagy, which appears to be selective and to degrade proteins in an ordered fashion and not completely arbitrarily as anticipated so far. *Molecular & Cellular Proteomics* 7: 2419–2428, 2008.**

Amino acid starvation is a physiological stimulus leading to numerous changes within the cell. Two of the major effects of starvation are a decreased protein synthesis and the activation of proteolytic pathways. The breakdown of proteins generates free amino acids that serve two functions: they are utilized for the *de novo* synthesis of proteins to support basic cellular functions and as substrates for the Krebs cycle to ensure cellular energy support (1). There are two main protein degradation routes in eukaryotic cells, the proteasomal and the lysosomal pathways. The proteasomal route is initiated by the ubiquitination of proteins that thereby are targeted for degradation by the proteasome (2). The ubiquitin-proteasome system is thought to be mainly responsible for the degradation of short lived proteins and defective ribosomal products (3). The lysosome, on the other hand, is the end point of multiple degradation pathways. Extracellular proteins are delivered to the lysosome by phagocytosis, pinocytosis, or re-

ceptor-mediated endocytosis. Intracellular components are delivered by chaperone-mediated autophagy (CMA)<sup>1</sup> (4), microautophagy (5), or macroautophagy (6, 7), hereafter referred to as autophagy.

Autophagy is responsible for cytoplasmic bulk degradation and thought to be important for the turnover of whole organelles and long lived proteins (8, 9). It is initiated by a flat membrane cistern enwrapping parts of the cytoplasm, thus forming autophagosomes with a characteristic double membraned organization. The autophagosome matures in a step-wise process that may involve fusion with endosomal vesicles (10) before it finally fuses with the lysosome leading to degradation of the autophagosomal material (6). Autophagy is induced upon cellular stress, such as starvation, organelle damage, pathogen invasion, and oxidative stress (11), and serves as a prosurvival response because mice with a defect in the autophagic response die upon neonatal starvation (12). In addition, stress-induced autophagy has been linked to several diseases, one of them being cancer. During the early phase of cancer development when tumors have not yet gained access to the blood system and thus have to survive in a nutrient-limited environment, autophagy may act as a pro-survival mechanism securing cellular energy needs (13, 14). On the other hand decreased autophagy has also been shown to increase tumorigenesis suggesting that at least under some circumstances autophagy can suppress tumor development (15, 16).

Autophagy is considered as an unselective bulk degradation pathway. However, lately selective types of autophagy have been described that lead to the elimination of specific organelles or protein aggregates (17), such as ER-phagy for ER-specific degradation (18), mitophagy for mitochondria-specific degradation (19), and ribophagy for ribosome-specific degradation (20). This raises the question whether regular autophagy is truly unselective. An unselective autophagic re-

From the <sup>‡</sup>Center of Experimental Bioinformatics, Department of Biochemistry and Molecular Biology, University of Southern Denmark, Campusvej 55, 5230 Odense, Denmark and <sup>¶</sup>Apoptosis Department and Center for Genotoxic Stress Research, Danish Cancer Society, Strandboulevarden 49, 2100 Copenhagen, Denmark

Received, April 24, 2008, and in revised form, July 10, 2008

Published, MCP Papers in Press, August 6, 2008, DOI 10.1074/mcp.M800184-MCP200

<sup>1</sup> The abbreviations used are: CMA, chaperone-mediated autophagy; 3-MA, 3-methyladenine; CTS, cathepsin; eGFP-LC3, enhanced green fluorescence protein light chain 3; ER, endoplasmic reticulum; FRAP1, FK506-binding protein 12 rapamycin-associated protein 1; GO, Gene Ontology; KEGG, Kyoto Encyclopedia of Genes and Genomes; mTOR, mammalian target of rapamycin; SILAC, stable isotope labeling by amino acids in cell culture; bis-Tris, 2-[bis(2-hydroxyethyl)amino]-2-(hydroxymethyl)propane-1,3-diol; STAGE, stop and go extraction; MSIP, International Protein Index specialized for mass spectrometry.

sponse during a starvation period could lead *e.g.* to the loss of too many mitochondria, which would additionally threaten cellular survival. Thus, it is plausible to hypothesize that autophagy is less unspecific than so far anticipated.

To study substrate selectivity of autophagy, we measured the relative abundance of proteins in the cell during amino acid starvation on a proteome scale. As responses to starvation are very complex we decided to keep glucose (1 g/liter) and serum (0%) levels constant. For the experiments we used MS-based quantitative proteomics in combination with stable isotope labeling by amino acids in cell culture (SILAC) (21). This method has already been used successfully to describe spatiotemporal dynamics of endogenous proteins (22, 23). We analyzed protein dynamics during a starvation period of 36 h and found that the subcellular localization of proteins had an influence on their degradation dynamics. Proteins were degraded in an ordered fashion in which cytosolic proteins and proteins involved in translation were degraded initially followed by multiprotein complexes and proteins situated in organelles. Autophagy was mainly responsible for this cellular phenomenon as validated by confocal imaging. Thus, our data imply that protein degradation during starvation-induced autophagy is regulated at the protein complex/organelle level and happens in an ordered fashion.

### EXPERIMENTAL PROCEDURES

**Cell Culture**—MCF7-eGFP-LC3 cells (24) were cultured in Dulbecco's modified Eagle's medium (Invitrogen) supplemented with 100 units/ml penicillin, 100  $\mu$ g/ml streptomycin, glutamine, 10% dialyzed fetal calf serum (Invitrogen) and labeled with either L-arginine and L-lysine, L-[U- $^{13}$ C<sub>6</sub>,  $^{14}$ N<sub>4</sub>]arginine and L-[ $^2$ H<sub>4</sub>]lysine, or L-[U- $^{13}$ C<sub>6</sub>,  $^{15}$ N<sub>4</sub>]arginine and L-[U- $^{13}$ C<sub>6</sub>,  $^{15}$ N<sub>2</sub>]lysine (Cambridge Isotope Laboratories, Andover, MA; Sigma-Aldrich) (2  $\times$  15-cm cell culture dishes per condition;  $\sim$ 95% confluent). Cells were washed three times in PBS before they were amino acid-starved in Hanks' balanced salt solution containing calcium, magnesium, and 1 g of sucrose/liter (Invitrogen) for 0, 6, and 18 h, respectively. A second identically labeled set of MCF7 cells was starved for 3, 6, and 36 h. All cell populations were serum-starved for 36 h in total (serum + amino acid starvation), and all treatments were carried out at 37 °C. The cells were scraped in cell scraping buffer (0.25 M sucrose, 1 mM sodium *ortho*-vanadate, 5 mM NaF, 5 mM  $\beta$ -glycerophosphate, and protease inhibitor mixture (Complete™ tablets, Roche Diagnostics)) and normalized by cell counting, and the 6-h amino acid-starved [ $^{13}$ C<sub>6</sub>]Arg/[ $^2$ H<sub>4</sub>]Lys cells served as a common reference point. To inhibit the different degradation pathways during 12-h amino acid starvation (2  $\times$  15-cm cell culture plates per condition; 95% confluent) the following inhibitors were used (all from Sigma-Aldrich): MG132 (1  $\mu$ M), epoxomicin (2  $\mu$ M), and 3-methyladenine (10 mM).

Mixed cells were centrifuged for 5 min at 1800 rpm and lysed in 6 M urea and 2 M thiourea, and 2% Benzoinase (Merck) was added before samples were concentrated on spin tubes (cutoff, 500 Da). Protein mixtures were separated by SDS-PAGE (4–12% bis-Tris gradient gel, NuPAGE, Invitrogen), gel lanes were cut into 15 slices, samples were in-gel digested (25), and resulting peptide mixtures were STAGE-tipped as described (26).

**Confocal Microscopy**—Cells were grown on coverslips as described above and rinsed three times with PBS before they were fixed in 3.7% paraformaldehyde for 15 min. Coverslips were mounted on

glass slides and imaged using a Zeiss LSM 510 Meta laser-scanning confocal microscope. For colocalization analyses cells were analyzed by live cell imaging using a POCmini-Chamber-System (LaCon, Staig, Germany). MitoTracker red and LysoTracker green were used according to the manufacturer's recommendations (Molecular Probes, Leiden, Netherlands). Each experiment was performed as two biological replicates, and three pictures were taken per experiment. Autophagosomes were counted with Image J software where an area between 0.07 and 0.65  $\mu$ m<sup>2</sup> was set.

**Mass Spectrometry**—Peptide mixtures eluted from STAGE tips were analyzed by on-line C<sub>18</sub> reversed-phase nanoscale liquid chromatography tandem mass spectrometry essentially as described previously (27) with a few modifications. Briefly experiments were performed on an Agilent 1100 nanoflow system (Agilent Technologies, Boeblingen, Germany) coupled to a linear ion trap Fourier transform ion cyclotron mass spectrometer (LTQ-FT-ICR Ultra, Thermo Fisher Scientific, Bremen, Germany) equipped with a nanoelectrospray ion source (Proxeon Biosystems, Odense, Denmark). The LTQ-FT-ICR Ultra was operated in data-dependent mode. For each cycle, a survey spectrum of 3  $\times$  10<sup>6</sup> ions between *m/z* 350 and 1600 was measured at a resolution of 100,000. In the linear ion trap, tandem mass spectra of the five most abundant multiply charged ions were recorded using a collision energy of 30% and a target value of 30,000. Mass spectrometric parameters were as follows: spray voltage, 2.3 kV; no sheath and auxiliary gas flow; ion transfer tube temperature, 150 °C.

**Assigning Peptide Sequences Using MASCOT and Quantitation Using MSQuant**—Raw MS2 spectra were centroided and merged into a single peak list file using the in-house-developed software DTAS-upercharge (default values; version 1.18) (44) and searched against the human MSIP database (version 3.28, 68688 entries; 3.32, 68,404 entries; 3.34, 68,174 entries) (28) using MASCOT 2.0 (Matrix Science, London, UK) with the following parameters: carbamidomethylcysteine was set as fixed modification and methionine oxidation, deamidation of asparagine and glutamine, and protein amino-terminal acetylation were set as variable modifications. Triple SILAC was chosen as quantification mode. Two miss cleavages were allowed, enzyme specificity was trypsin D/DP, precursor mass accuracy had to be within 30 ppm, and the fragment spectra mass accuracy was set at 0.8 Da. The identified peptides were recalibrated using MSQuant (version 1.4.3a89) (44), results were combined using MGF combiner (version 1.05) and re-searched using MASCOT 2.0 with the above mentioned parameters except that the precursor mass tolerance was set to 5 ppm. To determine the number of false-positive peptide hits the data were searched against a human MSIP decoy database essentially as described previously (29), and the MASCOT peptide score was adjusted to yield a number of false-positive (FP) peptide identifications of less than 1% (calculated as follows: FP rate (%) = reverse hits  $\times$  2  $\times$  100/forward hits). For a protein to be counted as identified a minimum of two unique peptides (bold red hits; minimum length, 7 amino acids) had to be sequenced and had to fulfill the determined criteria. Peptides were quantified by MSQuant using extracted ion chromatograms of the monoisotopic signals. Protein ratios were normalized so that the identified histone ratios were 1:1:1. For cluster analyses, protein ratios were normalized to 0 (calculated as  $x - 1$  for protein ratios larger than 1 and  $1 - (1/x)$  for protein ratios smaller than 1).

**Data Analysis**—Proteins were clustered using The Institute of Genomic Research MultiExperiment Viewer (TM4) software (30). A self-organizing tree algorithm was used with the following settings: Euclidian distance as matrix with five cycles and cell variability of 0.05. The preservation of important information about the magnitude of change is at the expense of outliers causing undesired correlations between genes. Therefore, four outliers were temporarily removed and afterward manually added to cluster A. High throughput GoMiner

(31) was used to investigate the Gene Ontology (GO) identities of proteins in the generated clusters and the regulated proteins in the inhibitor studies. Protein Center (Proxeon Biosystems) was used to combine redundant protein hits with 98% homology between several data sets and to analyze subcellular localizations. Babelomics was used to analyze KEGG pathways. Two biological replicates were analyzed showing essentially the same results.

A search for KFERQ-like motifs in all observed proteins was based on a 2-fold analysis of (a) all experimentally observed KFERQ-like motifs (including reverse motifs) and (b) a search based on all possible combinations of the basic patterns (1143 motifs) matching the very basic motif description supplied previously (32). The distribution of N-terminal amino acids (after removal of N-terminal methionine) in each cluster was analyzed to test whether the observed degradation patterns confer with the N-end rule where the N-terminal amino acid determines the lifespan of the protein.

## RESULTS

**Protein Dynamics during Amino Acid Starvation**—To follow starvation-induced protein dynamics on a proteome scale the following SILAC experiment (21) was performed. Three populations of MCF7 cells were SILAC-encoded with both arginine and lysine using three distinct isotope forms. After complete isotope incorporation the cells were amino acid-starved for different time periods, whereas the length of serum starvation was kept constant. The presence of 1 g/liter glucose allowed maximum cell survival under these stress conditions. Two time course experiments were combined using 6 h of amino acid starvation as a common time point, providing a five-time point profile (Fig. 1A). Subsequently cells were mixed and lysed, and proteins were separated by SDS-PAGE prior to in-gel digestion (25) and on-line LC-MS on a hybrid linear ion trap/Fourier transform ion cyclotron resonance mass spectrometer (LTQ-FT-ICR Ultra). All labeled peptides elute as triplets where the intensities reflect the relative amount of peptide at the corresponding time points (Fig. 1B). Quantitation was done by our in-house-developed software MSQuant yielding an average relative S.D. of 13%. As starvation leads to a cell cycle arrest (33), we assumed that proteins involved in DNA organization should stay constant during the analyzed time frame. Therefore, histones were used to normalize the data to a mixing ratio of 1:1:1. Fig. 1C shows examples of recorded and normalized profiles of proteins changing in abundance over the analyzed starvation period.

Altogether we were able to record 1486 protein profiles consisting of five time points each (supplemental Table 1) that were clustered by a self-organizing tree algorithm using Euclidian distance as matrix. Six clusters were generated as shown in Fig. 2, A–F. The first five clusters contain proteins decreasing with different kinetics (*blue*), and the last cluster contains proteins that stayed constant or increased (*yellow*). We observed a strong decrease of proteins involved in translation, such as ribosomal protein S6 (Fig. 1C), which located to cluster A. Interestingly we also detected a decrease of its upstream kinase mammalian target of rapamycin (mTOR)

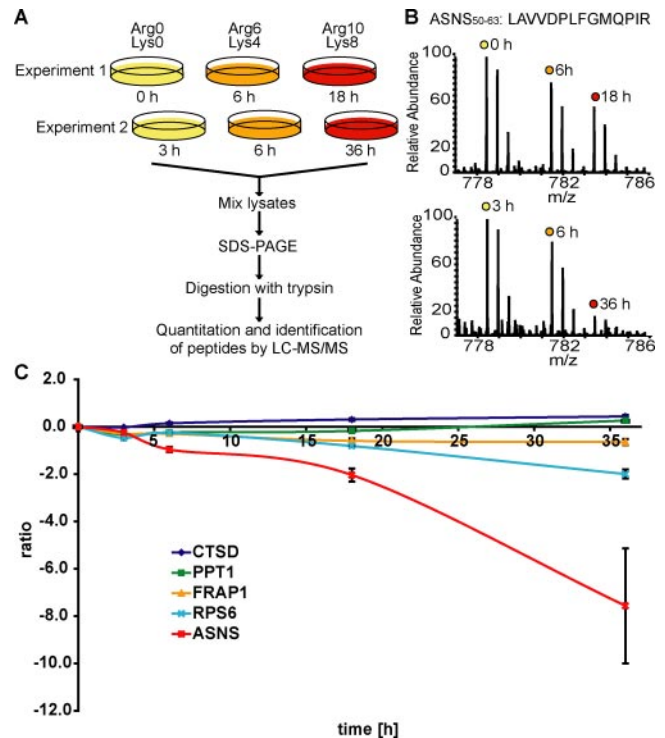


**FIG. 1. Protein dynamics during amino acid starvation.** A, a quantitative MS experiment was designed using SILAC and treatment of cells for different time periods. Cells were SILAC-labeled and starved for 0, 6, and 18 h or 3, 6, and 36 h. Subsequently cells from one experiment were combined and lysed. The protein content was separated by SDS-PAGE and digested by trypsin, and the resulting peptide mixtures were analyzed by LC-MS/MS. B, labeling of cells resulted in peptide triplets, their intensities reflecting the relative amount at the corresponding time points. A five-time point profile was generated using 6 h as common value. C, protein profiles of five selected proteins with respective relative S.D. (shown as error bars). Most proteins decreased, such as asparagine synthetase (ASNS), mTOR (FRAP1), and its downstream effector ribosomal protein S6 (RPS6). Only a few proteins increased, e.g. CTSD and palmitoyl-protein thioesterase 1 (PPT1).

(FRAP1; Fig. 1C), which is known to be inhibited during starvation conditions (34). Furthermore we noticed a strong decrease in the amount of tRNA synthetases: 11 of the 17 detected were located in clusters A and B containing proteins decreasing very early during starvation.

To investigate whether the subcellular localization of proteins had an influence on their degradation dynamics, we analyzed the distribution of proteins from specific multiprotein complexes and organelles according to GO (35) using the software GoMiner and Protein Center. As multiple GO terms can be assigned to one protein results have to be interpreted carefully. Although we did not detect the entire proteome, we detected at least 10 proteins per analyzed organelle (on average 48 proteins per organelle), which represents an adequate coverage of organellar proteins to draw biological conclusions. To our surprise, we observed a correlation between the degradation profiles of proteins and their subcellular lo-

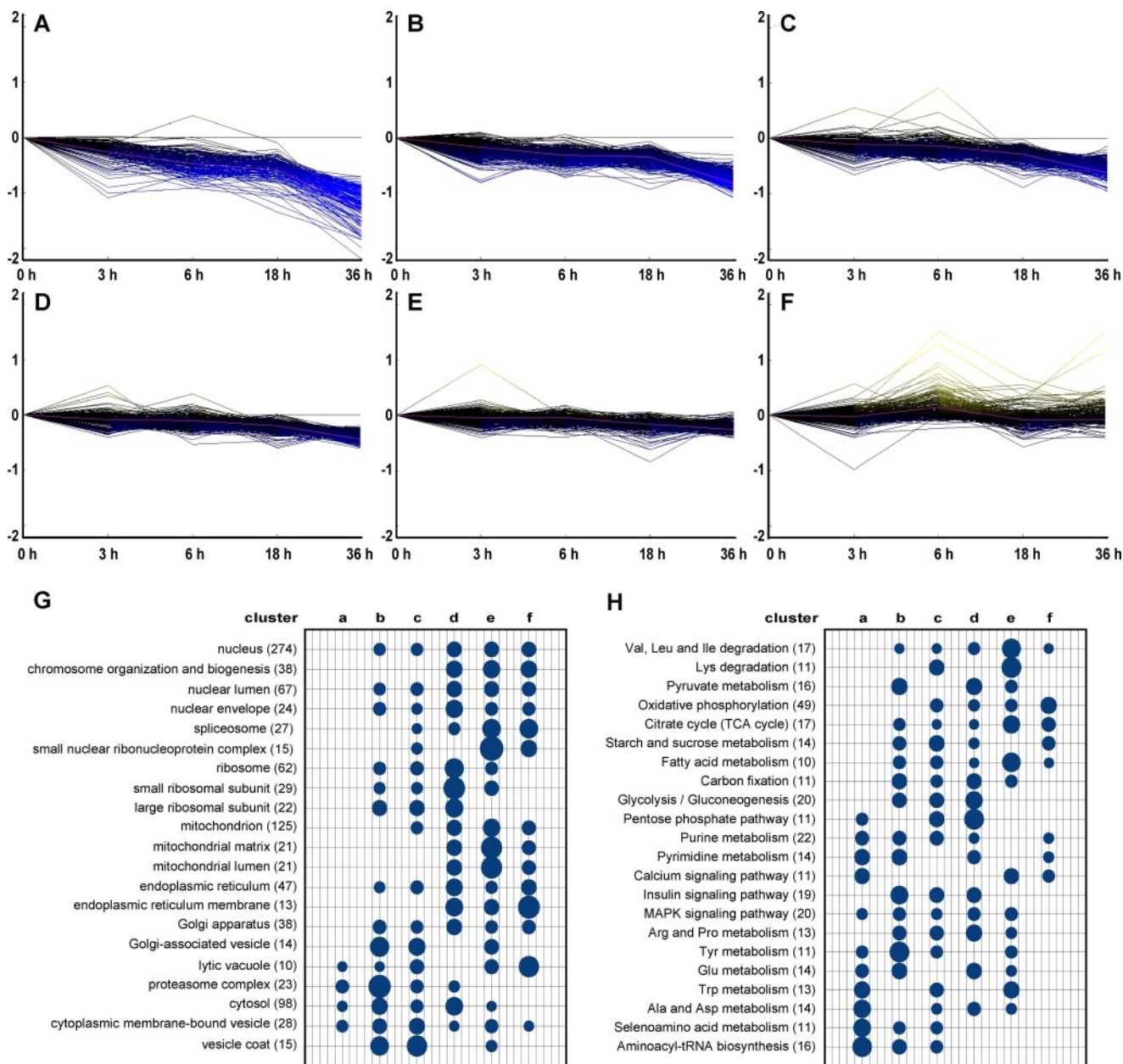


**FIG. 2. Cluster analysis of recorded protein profiles.** A–F, clusters were generated by a self-organizing tree algorithm using Euclidian distance as a matrix (The Institute of Genomic Research TM4 software). Clusters contain 155 (A), 287 (B), 283 (C), 276 (D), 269 (E), and 212 (F) protein profiles. Blue marks decreasing proteins; yellow marks increasing ones. The red line shows the average profile of each cluster. G, proteins were grouped according to their subcellular localization (numbers in parentheses indicate the number of identified proteins). The sizes of the dots represent the percentage of each group assigned to a specific cluster (10% cutoff value). H, proteins were grouped according to their KEGG pathways (numbers in parentheses indicate the number of identified proteins). The sizes of the dots represent the percentage of each group assigned to a specific cluster (10% cutoff value). TCA, tricarboxylic acid; MAPK, mitogen-activated protein kinase.

calization (Fig. 2G, supplemental Table 2, and supplemental Fig. 1). Free cytosolic proteins were rapidly degraded and located mainly in clusters A and B. The large fraction of cytosolic proteins in cluster D was due to ribosomal proteins that also carry the GO term cytosolic. Proteasomal proteins were similarly rapidly degraded and located largely in cluster B. Ribosomal proteins localized to cluster D and showed already a delayed degradation profile. Mitochondrial proteins lo-

cated mainly in cluster E. As anticipated, nuclear proteins were relatively stable with 42% localized in clusters E and F as compared with 21% in clusters A and B. One-third of the nuclear proteins localized in the first two clusters were also annotated as cytosolic compared with only 10% in clusters E and F, indicating that this group belonged to rapidly degraded cytosolic proteins. Dynamic organelles involved in vesicular transport such as the Golgi apparatus, the ER, and the vacuole

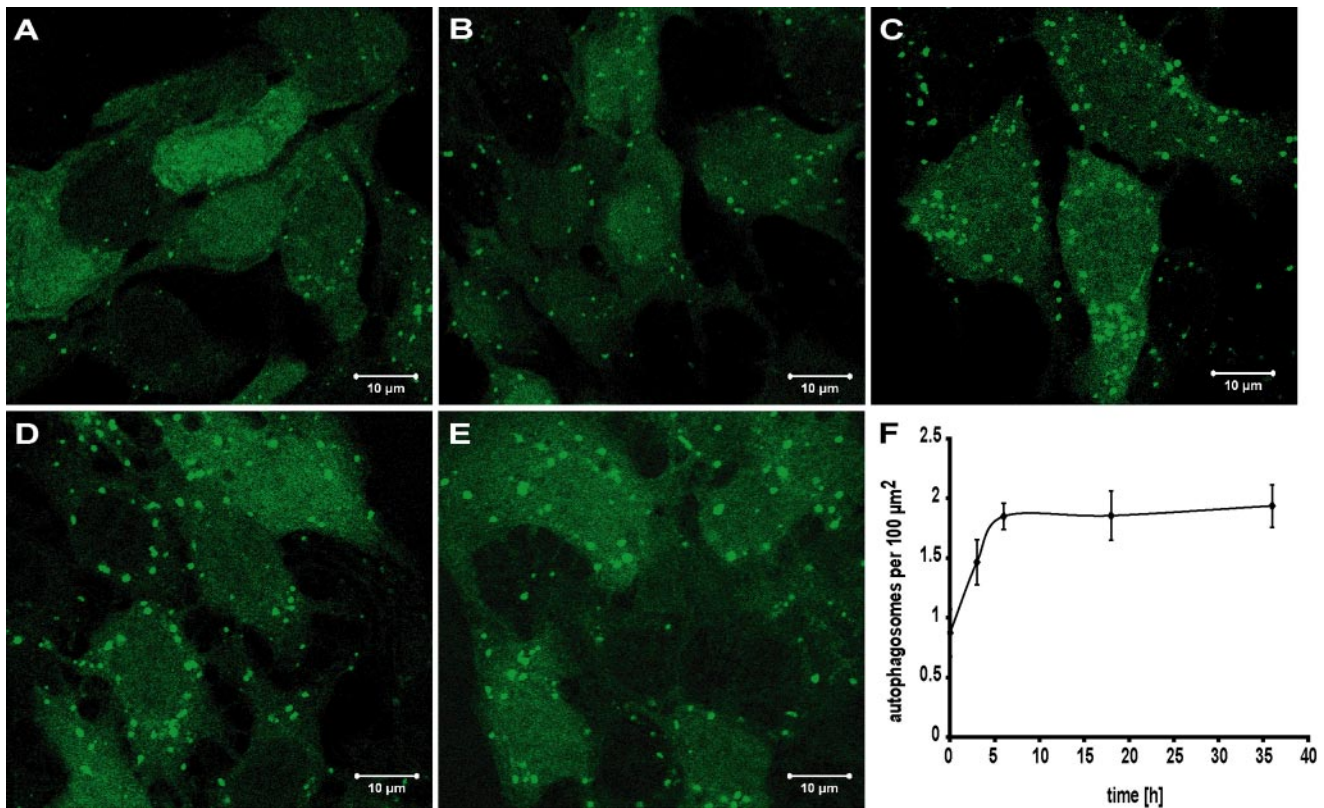


**FIG. 3. Accumulations of autophagosomes during amino acid starvation.** MCF7-eGFP-LC3 cells were starved in Hanks' balanced salt solution for 0 (A), 3 (B), 6 (C), 18 (D), and 36 h (E). The accumulation of autophagosomes was visualized by translocation of eGFP-LC3 into dotted structures (autophagosomes). F, after 6 h of starvation a steady-state level of autophagosomes is reached with  $\sim 2/100 \mu\text{m}^2$  cell area.

were difficult to address as their proteins generally carry multiple GO terms and can localize in different subcellular compartments. Proteins staying at a constant level during starvation localized to cluster F that contained e.g. ER membrane and spliceosomal proteins. A large fraction of vacuolar proteins involved in degradation processes was also found in cluster F, e.g. hexosaminidase B, palmitoyl-protein thioesterase 1, cathepsins D and B (CTSD and CTSB). The last three showed even a slight increase over time (Fig. 1C). Thus, compared with proteasomal proteins, which drop dramatically, some lysosomal proteases stay constant or increase, highlighting their importance during amino acid starvation and indicating that proteins are most likely degraded in the lysosome under such conditions in MCF7 cells. In a biological replicate 1133 proteins were quantified, and organelles showed very similar degradation characteristics (supplemental Fig. 2).

We also investigated whether certain biological processes were overrepresented in the different clusters according to the corresponding KEGG pathway annotations. For example, aminoacyl-tRNA biosynthesis and purine and pyrimidine metabolism located mainly in clusters A and B, whereas the Krebs cycle ended primarily in clusters E and F, supporting our findings regarding the different degradation kinetics of proteins from distinct subcellular localizations (Fig. 2H and supplemental Table 3).

**Amino Acid Starvation-induced Autophagy**—The two major intracellular eukaryotic protein degradation pathways are the ubiquitin-proteasome system and the autophagosomal/lysosomal system. The proteasome seemed to play only a minor role in protein degradation during starvation conditions in MCF7 cells as it localized mainly to cluster B, meaning it was rapidly degraded. In addition, we did not find any specific distribution of proteins in clusters in concordance with the N-end rule that states that proteins having a specific N terminus are especially prone to proteasomal degradation (supplemental Table 4) (36).

Autophagy is blocked by mTOR, which was degraded during the starvation period (Fig. 1C), and it is known that autophagy can be induced by starvation in MCF7 cells. To determine autophagy induction, we monitored the level of autophagosome accumulation during 36 h of amino acid starvation in MCF7 cells stably expressing the autophagosome-associated protein LC3 fused to enhanced green fluorescence protein (eGFP-LC3) (24). In control cells eGFP-LC3 stained diffusely in cytosol and nucleus. As expected, during the starvation period the number of dotted eGFP-LC3 increased indicating that autophagosomes were formed in the cells (Fig. 3, A–E). After 6 h a steady-state level of  $\sim 2$  autophagosomes/100- $\mu\text{m}^2$  cell area was reached (Fig. 3F).

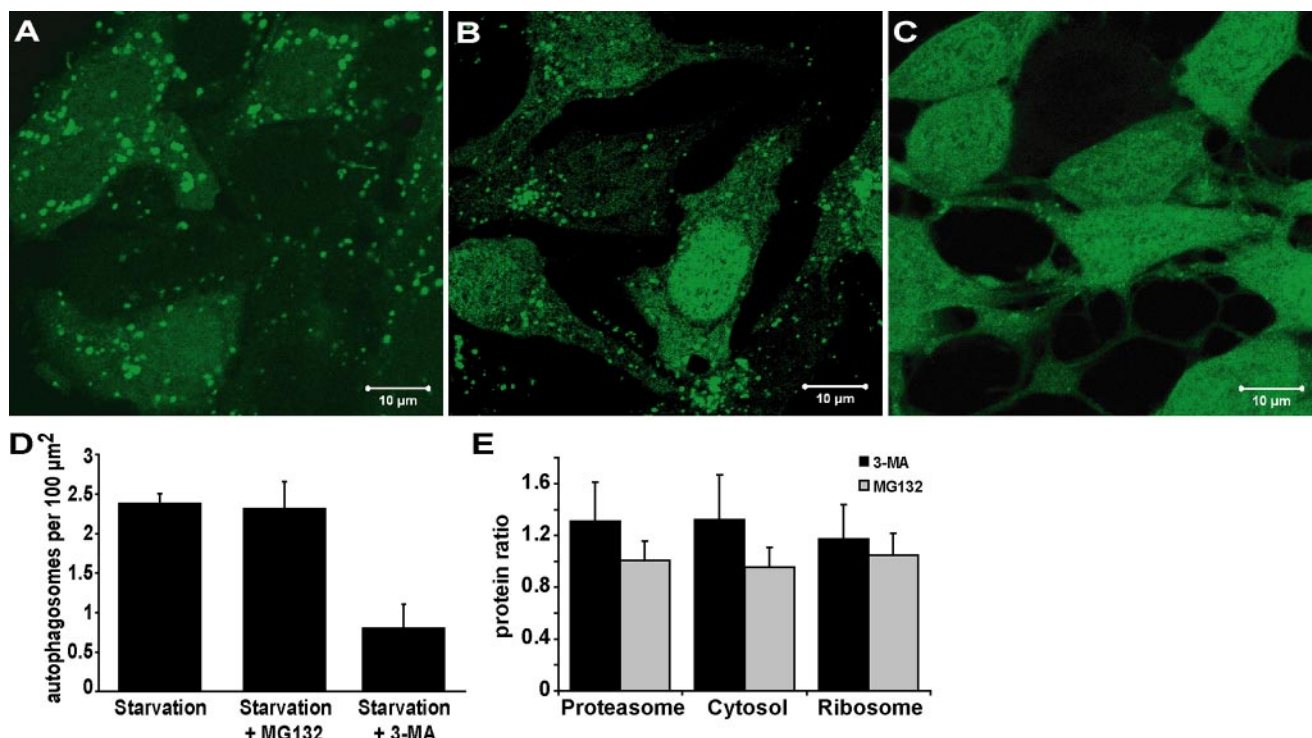


**FIG. 4. Inhibition of degradation pathways.** Induction of autophagy during 12 h of amino acid starvation was assessed by autophagosome accumulation using MCF7-eGFP-LC3 cells. *A*, starved control cells were compared with starved cells additionally treated with 1  $\mu\text{M}$  MG132 (*B*) and 10 mM 3-MA (*C*). *D*, the autophagosomal inhibitor 3-MA suppressed autophagosome generation. MG132, a proteasome inhibitor, had no significant effect on autophagosome number. *E*, proteins were grouped according to their subcellular localization and quantified. Depicted are the mean ratios of proteins in each group with the corresponding S.D. Upon application of unpaired two-tail Student's *t* tests to the groups of quantified proteins, the means turned out to be significantly different ( $p < 0.001$ ). Blocking the autophagic process by 3-MA during amino acid starvation did not lead to an increase in cell death in the investigated time frame.

**Inhibition of Protein Degradation Pathways**—To investigate the importance of the proteasomal and the autophagosomal/lysosomal degradation routes during starvation conditions we inhibited both pathways by drugs, hypothesizing that proteins being degraded by one specific pathway should increase if the respective pathway is blocked. Thus, we inhibited the proteasome by MG132 and autophagy by 3-methyladenine (3-MA) for a 12-h starvation period. The number of autophagosomes from cells treated with the proteasomal inhibitor did not differ significantly compared with starved cells (Fig. 4, *A*, *B*, and *D*). 3-MA inhibits class III phosphatidylinositol 3-kinases, which are required for the initial nucleation and assembly of the primary autophagosomal membrane (37, 38). Accordingly 3-MA inhibited autophagosomal formation during amino acid starvation (Fig. 4, *C* and *D*).

Protein degradation dynamics were analyzed by quantitative MS as follows. SILAC-encoded cells were starved for 12 h in the presence of the inhibitors and mixed with starved control cells. The combined cells were lysed, and lysates were processed as outlined in Fig. 1A. Looking at proteins that were degraded within the first 12 h of starvation in the initial study, namely cytosolic, proteasomal, and ribosomal proteins, it became evident that proteasome inhibition during amino acid starvation had hardly any effect on protein abun-

dance. The mean ratios of all three groups did reflect the mixing ratio of the experiment. The proteasomal inhibitor epoxomicin showed similar results (data not shown). On the other hand inhibition of autophagy by 3-MA led to an increase of proteins from all three localizations (Fig. 4*E* and supplemental Tables 5 and 6). The means of cytosolic and proteasomal protein abundance rose over 30%, and the mean of ribosomal protein abundance rose over 17%. Upon application of unpaired two-tail Student's *t* tests to the groups of quantified proteins, the means turned out to be significantly different ( $p < 0.001$ ). Thus, as already mentioned in the preceding paragraph, it appears that proteasomal degradation during starvation conditions in MCF7 cells is less important than autophagosomal/lysosomal degradation.

As autophagy appeared to be the major degradation pathway during starvation conditions in MCF7 cells we wondered how the ordered nature of degradation we observed could be carried out by a process described as unspecific bulk degradation. One explanation could be that different types of autophagy are active at different time points during starvation. It has already been suggested that macroautophagy is only active during the initial starvation phase and that later CMA takes over (1). We recorded numerous profiles of proteins known to be CMA substrates, such as tRNA synthetases (4)

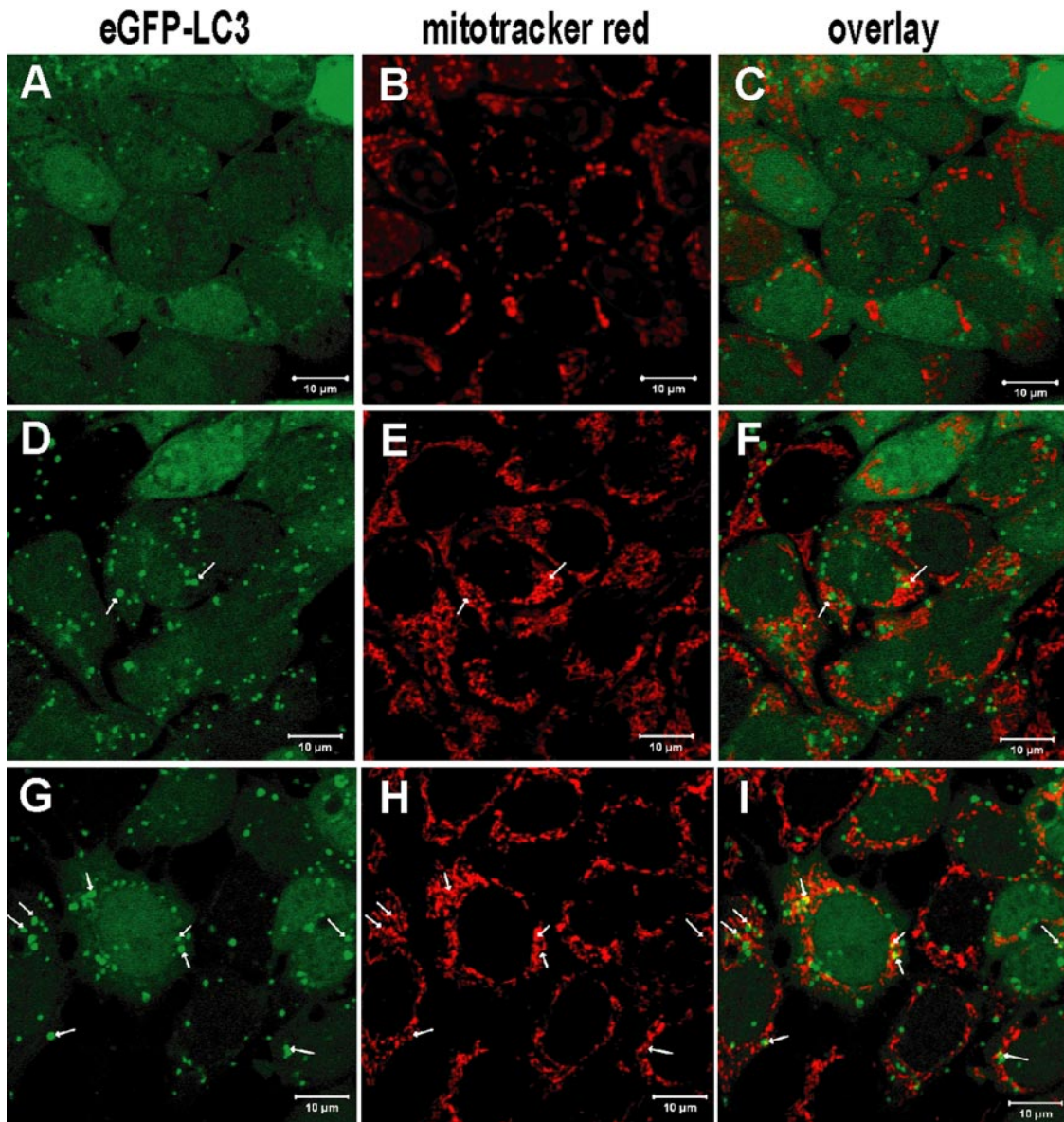


**FIG. 5. Mitochondrial/autophagosomal colocalization after long term starvation.** Mitochondrial elimination during amino acid starvation was analyzed by microscopy using MCF7-eGFP-LC3 cells and MitoTracker red. Whereas non-starved control cells did not show any mitochondrial/autophagosomal colocalization (A–C), we were able to detect a low level of colocalization after 7 h of starvation (D–F). However, after 30 h of starvation extensive mitochondrial/autophagosomal colocalization was visible (G–I). Arrows indicate major sites of colocalization.

and proteasomal proteins (39). However, in our case these proteins were rapidly degraded, indicating that CMA might play a role in the initial starvation period. To address the impact of CMA on the detected protein dynamics, we analyzed the occurrence of experimentally verified KFERQ-like motifs and the cluster distribution of the corresponding proteins. Substrates for CMA are reported to contain a pentapeptide motif related to the KFERQ sequence (4, 40). We did not find a correlation between protein profiles and the occurrence of KFERQ-like motifs. In fact, potential protein substrates of CMA localized to all six clusters (supplemental Table 7), indicating that CMA-dependent degradation cannot explain the

observed cluster distribution of proteins. Thus, macroautophagy itself appears to be responsible for the ordered nature of protein breakdown.

**Mitochondrial Degradation through Autophagy**—To further verify that autophagy is responsible for ordered organelle degradation, we followed the subcellular localization of mitochondria during amino acid starvation by microscopy. We compared cells amino acid-starved for 7 and 30 h with non-starved control cells (Fig. 5). Whereas we rarely detected mitochondrial-autophagosomal colocalization after 7 h of starvation (Fig. 5, D–F), we were able to detect extensive colocalization after 30 h (Fig. 5, G–I). The same

holds true for mitochondrial-lysosomal colocalization (supplemental Fig. 3, A–I). These observations are in accordance with already obtained results, highlighting that autophagy is regulated at the protein complex/organelle level and that organelles are degraded in an ordered fashion via autophagy in the lysosome.

DISCUSSION

Amino acid starvation represents the classical stimulus to induce macroautophagy, which is still considered to be an unspecific bulk degradation pathway (41). However, this hypothesis has been questioned numerous times as the unspecific elimination of vital organelles could threaten cellular survival. Already in 1986 Kitagawa and Ono (42) noticed that autophagosomes in rat pancreatic exocrine cells contained mitochondria and ER only after long term starvation. In addition, a selectivity toward the substrate ALD6P has been shown in yeast (43). We have analyzed protein degradation dynamics by quantitative MS under autophagic conditions in the human MCF7 breast carcinoma cell line and were able to record protein profiles of almost 1500 proteins consisting of five time points each. Cluster analysis of these profiles revealed that degradation dynamics strongly depend on the subcellular localization of the corresponding proteins. Cytosolic proteins, multiprotein complexes, and organelles showed distinct degradation patterns. Thus, we were able to show by an unbiased proteome-wide analysis that protein degradation during starvation-induced autophagy is regulated at the protein complex/organelle level and happens in an ordered fashion (Fig. 6).

Quantitative MS has become a very powerful tool to follow spatiotemporal dynamics of endogenous proteins and of protein modifications in different experimental settings (44). In the current work, we used SILAC (21) in combination with treatment of cell populations to globally follow protein degradation during amino acid starvation at multiple time points. To our knowledge, this is the most comprehensive data set on protein dynamics during starvation conditions so far. Cytosolic and proteasomal proteins were degraded rapidly followed by ribosomal proteins. On the other hand mitochondrial, ER, spliceosome, and vacuolar proteins lagged greatly behind. One reason for delayed organellar protein degradation could be that cytosolic proteins are more easily accessible than organellar proteins, which are part of larger structures and in many cases are integrated into membranes. Another reason could be that the cell “chooses” to degrade organelles at a later time point as they are energetically more expensive to synthesize and important for cellular survival. The idea of a selective process is supported by the fact that we were able to detect only minor mitochondrial/autophagosomal colocalization during the early phase of starvation, whereas we saw extensive colocalization at a later time point.

One of the major cellular responses to amino acid starvation is the initiation of autophagy. Autophagy is an evo-

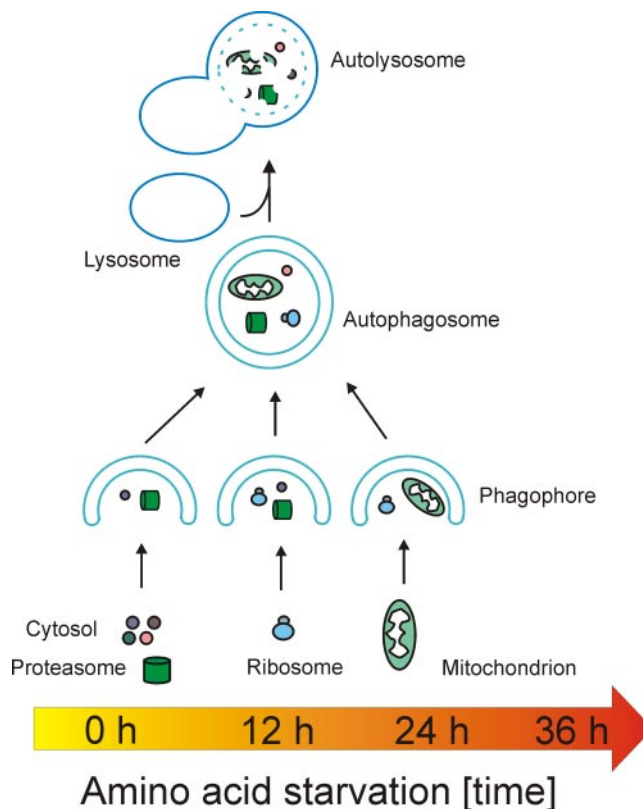


FIG. 6. **Model of protein degradation dynamics during starvation-induced autophagy.** Protein degradation during autophagy is ordered. Early during starvation cytosolic and proteasomal proteins are degraded in the lysosome via autophagy. Only at later time points do organelles, which are energetically more costly to synthesize, follow this route.

lutionarily conserved process thought to be important for the turnover of whole organelles and long lived proteins. However, prolonged autophagy can lead to type II programmed cell death. Autophagy has been linked to several diseases, ranging from myopathies, heart and liver diseases, and neurodegeneration to cancer (9, 45). In all cases autophagy has been described to have beneficial as well as detrimental effects, depending among others on the disease state. This highlights the complexity of autophagy regulation and the need to further define underlying processes. Using confocal microscopy, we detected an induction of autophagy during starvation in MCF7 cells by eGFP-LC3 translocation into autophagosomes that reached a steady-state level after 6 h. To delineate the cellular pathways responsible for protein degradation during amino acid starvation, we inhibited the proteasome and autophagy by drugs. Whereas the proteasome has been shown to be important for cellular survival during an acute decrease in the external amino acid supply (46), the autophagosomal-lysosomal pathway appears to be the major degradative route during long term starvation; this is highlighted by the increase of lysosomal proteases, glycosidases, and lipases.

Inhibition of the proteasome led only to minor changes in protein abundance. During autophagy inhibition we observed an increase of ribosomal, cytosolic, and proteasomal proteins, the latter two decreasing rapidly at the beginning of starvation. The strong increase during inhibited autophagy stresses its importance for the degradation of these protein groups.

As protein degradation happened primarily via the autophagosomal/lysosomal route we wanted to outline the influence of different autophagy subtypes and compared CMA with macroautophagy. CMA could not explain the observed cluster distribution of proteins during starvation. Thus, CMA seems to play only a minor role during amino acid starvation in MCF7 cells. However, we cannot exclude that CMA is responsible for the degradation dynamics of single proteins. The ordered nature of protein degradation observed during amino acid starvation could also be influenced by steric properties/hindrance of the respective substrates. Thus, smaller substrates could be degraded rapidly, whereas larger substrates would be delayed. We analyzed the size distribution of proteins in each cluster and did not observe major differences, although the largest substrates localized to clusters E and F. A likely explanation for this could be the general size difference between cytosolic and nuclear proteins. In general, the majority of proteins in each cluster had a length of 200–400 amino acid residues (supplemental Fig. 4). Organelle-specific autophagy types such as ER-phagy (18) and mitophagy (19) could influence the ordered nature of degradation. One could imagine that organelle-specific degradation is initiated at specific time points, which would yield the observed protein profiles. Further we would like to point out that we also detected distinct degradation patterns for different multiprotein complexes resident in the cytosol, such as the proteasome and the ribosome. In addition, protein groups such as tRNA synthetases also showed distinct degradation profiles. This all indicates that autophagy is much more tightly regulated as so far anticipated and that proteins are not arbitrarily degraded via this pathway. Tightly regulated macroautophagy or temporally regulated autophagy subtypes could be responsible for this phenomenon. Future work to delineate underlying mechanisms of substrate specificity of autophagy could help to solve this problem.

Taken together, we have generated a comprehensive data set of cellular protein dynamics during 36 h of amino acid starvation. In an unbiased approach we were able to highlight that proteins with different subcellular localizations show distinct degradation patterns and that degradation is mainly dependent on the autophagosomal/lysosomal pathway. Thus, starvation-induced autophagy seems to be selective and to degrade proteins in an ordered fashion and not in a completely unspecific bulk process. Our study raises the important questions of how the autophagosome decides what to take up and to deliver to the lysosome and how these choices change over time.

**Acknowledgments**—The Center of Experimental Bioinformatics (CEBI) is supported by a generous grant from the Danish National Research Foundation. We thank all CEBI group members for helpful discussions and support, especially B. Blagoev, V. Akimov, P. Mortensen, M. Nielsen, and K. Rigbolt.

\* This work was supported in part by the collaborative project Apo-Sys under the European Union FP7 program and by the Danish Cancer Society, which supported the work within the project: spatio-temporal proteomics of autophagy in cancer cells. The costs of publication of this article were defrayed in part by the payment of page charges. This article must therefore be hereby marked “advertisement” in accordance with 18 U.S.C. Section 1734 solely to indicate this fact.

☒ The on-line version of this article (available at <http://www.mcponline.org>) contains supplemental material.

§ Supported by the Danish Cancer Society.

|| Both authors contributed equally to this work.

\*\* Supported by the European Molecular Biology Organization. To whom correspondence may be addressed. Tel.: 45-6550-2365; Fax: 45-6593-3018; E-mail: [dengjel@bmb.sdu.dk](mailto:dengjel@bmb.sdu.dk).

‡‡ To whom correspondence may be addressed. Tel.: 45-6550-2365; Fax: 45-6593-3018; E-mail: [jens.andersen@bmb.sdu.dk](mailto:jens.andersen@bmb.sdu.dk).

#### REFERENCES

1. Finn, P. F., and Dice, J. F. (2006) Proteolytic and lipolytic responses to starvation. *Nutrition* **22**, 830–844
2. Ciechanover, A. (2005) Proteolysis: from the lysosome to ubiquitin and the proteasome. *Nat. Rev. Mol. Cell Biol.* **6**, 79–87
3. Princiotta, M. F., Finzi, D., Qian, S. B., Gibbs, J., Schuchmann, S., Buttgerit, F., Binnink, J. R., and Yewdell, J. W. (2003) Quantitating protein synthesis, degradation, and endogenous antigen processing. *Immunity* **18**, 343–354
4. Dice, J. F. (2007) Chaperone-mediated autophagy. *Autophagy* **3**, 295–299
5. Klionsky, D. J., Cuervo, A. M., and Seglen, P. O. (2007) Methods for monitoring autophagy from yeast to human. *Autophagy* **3**, 181–206
6. Kroemer, G., and Jaattela, M. (2005) Lysosomes and autophagy in cell death control. *Nat. Rev. Cancer* **5**, 886–897
7. Yorimitsu, T., and Klionsky, D. J. (2005) Autophagy: molecular machinery for self-eating. *Cell Death Differ.* **12**, Suppl. 2, 1542–1552
8. Henell, F., Berkenstam, A., Ahlberg, J., and Glaumann, H. (1987) Degradation of short- and long-lived proteins in perfused liver and in isolated autophagic vacuoles-lysosomes. *Exp. Mol. Pathol.* **46**, 1–14
9. Mizushima, N., Levine, B., Cuervo, A. M., and Klionsky, D. J. (2008) Autophagy fights disease through cellular self-digestion. *Nature* **451**, 1069–1075
10. Gordon, P. B., and Seglen, P. O. (1988) Prelysosomal convergence of autophagic and endocytic pathways. *Biochem. Biophys. Res. Commun.* **151**, 40–47
11. De Duve, C., and Wattiaux, R. (1966) Functions of lysosomes. *Annu. Rev. Physiol.* **28**, 435–492
12. Kuma, A., Hatano, M., Matsui, M., Yamamoto, A., Nakaya, H., Yoshimori, T., Ohsumi, Y., Tokuhiya, T., and Mizushima, N. (2004) The role of autophagy during the early neonatal starvation period. *Nature* **432**, 1032–1036
13. Levine, B. (2007) Cell biology: autophagy and cancer. *Nature* **446**, 745–747
14. Mathew, R., Karantza-Wadsworth, V., and White, E. (2007) Role of autophagy in cancer. *Nat. Rev. Cancer* **7**, 961–967
15. Mathew, R., Kongara, S., Beaudoin, B., Karp, C. M., Bray, K., Degenhardt, K., Chen, G., Jin, S., and White, E. (2007) Autophagy suppresses tumor progression by limiting chromosomal instability. *Genes Dev.* **21**, 1367–1381
16. Pattingre, S., and Levine, B. (2006) Bcl-2 inhibition of autophagy: a new route to cancer? *Cancer Res.* **66**, 2885–2888
17. van der Vaart, A., Mari, M., and Reggiori, F. (2008) A picky eater: exploring the mechanisms of selective autophagy in human pathologies. *Traffic* **9**, 281–289
18. Bernales, S., McDonald, K. L., and Walter, P. (2006) Autophagy counterbalances endoplasmic reticulum expansion during the unfolded protein

- response. *PLoS Biol.* **4**, e423
19. Kim, I., Rodriguez-Enriquez, S., and Lemasters, J. J. (2007) Selective degradation of mitochondria by mitophagy. *Arch. Biochem. Biophys.* **462**, 245–253
  20. Kraft, C., Deplazes, A., Sohrmann, M., and Peter, M. (2008) Mature ribosomes are selectively degraded upon starvation by an autophagy pathway requiring the Ubp3p/Bre5p ubiquitin protease. *Nat. Cell Biol.* **10**, 602–610
  21. Ong, S. E., Blagoev, B., Kratchmarova, I., Kristensen, D. B., Steen, H., Pandey, A., and Mann, M. (2002) Stable isotope labeling by amino acids in cell culture, SILAC, as a simple and accurate approach to expression proteomics. *Mol. Cell. Proteomics* **1**, 376–386
  22. Andersen, J. S., Lam, Y. W., Leung, A. K., Ong, S. E., Lyon, C. E., Lamond, A. I., and Mann, M. (2005) Nucleolar proteome dynamics. *Nature* **433**, 77–83
  23. Blagoev, B., Ong, S. E., Kratchmarova, I., and Mann, M. (2004) Temporal analysis of phosphotyrosine-dependent signaling networks by quantitative proteomics. *Nat. Biotechnol.* **22**, 1139–1145
  24. Hoyer-Hansen, M., Bastholm, L., Szyniarowski, P., Campanella, M., Szabadkai, G., Farkas, T., Bianchi, K., Fehrenbacher, N., Elling, F., Rizzuto, R., Mathiasen, I. S., and Jaattela, M. (2007) Control of macroautophagy by calcium, calmodulin-dependent kinase kinase- $\beta$ , and Bcl-2. *Mol. Cell* **25**, 193–205
  25. Shevchenko, A., Tomas, H., Havlis, J., Olsen, J. V., and Mann, M. (2006) In-gel digestion for mass spectrometric characterization of proteins and proteomes. *Nat. Protoc.* **1**, 2856–2860
  26. Rappsilber, J., Ishihama, Y., and Mann, M. (2003) Stop and go extraction tips for matrix-assisted laser desorption/ionization, nanoelectrospray, and LC/MS sample pretreatment in proteomics. *Anal. Chem.* **75**, 663–670
  27. Gruhler, A., Olsen, J. V., Mohammed, S., Mortensen, P., Faergeman, N. J., Mann, M., and Jensen, O. N. (2005) Quantitative phosphoproteomics applied to the yeast pheromone signaling pathway. *Mol. Cell. Proteomics* **4**, 310–327
  28. Schandorff, S., Olsen, J. V., Bunkenborg, J., Blagoev, B., Zhang, Y., Andersen, J. S., and Mann, M. (2007) A mass spectrometry-friendly database for cSNP identification. *Nat. Methods* **4**, 465–466
  29. Elias, J. E., Gibbons, F. D., King, O. D., Roth, F. P., and Gygi, S. P. (2004) Intensity-based protein identification by machine learning from a library of tandem mass spectra. *Nat. Biotechnol.* **22**, 214–219
  30. Saeed, A. I., Sharov, V., White, J., Li, J., Liang, W., Bhagabati, N., Braisted, J., Klapa, M., Currier, T., Thiagarajan, M., Sturn, A., Snuffin, M., Rezantsev, A., Popov, D., Ryltsov, A., Kostukovich, E., Borisovsky, I., Liu, Z., Vinsavich, A., Trush, V., and Quackenbush, J. (2003) TM4: a free, open-source system for microarray data management and analysis. *BioTechniques* **34**, 374–378
  31. Zeeberg, B. R., Qin, H., Narasimhan, S., Sunshine, M., Cao, H., Kane, D. W., Reimers, M., Stephens, R. M., Bryant, D., Burt, S. K., Enekave, E., Hari, D. M., Wynn, T. A., Cunningham-Rundles, C., Stewart, D. M., Nelson, D., and Weinstein, J. N. (2005) High-throughput GoMiner, an 'industrial-strength' integrative gene ontology tool for interpretation of multiple-microarray experiments, with application to studies of common variable immune deficiency (CVID). *BMC Bioinformatics* **6**, 168
  32. Majeski, A. E., and Dice, J. F. (2004) Mechanisms of chaperone-mediated autophagy. *Int. J. Biochem. Cell Biol.* **36**, 2435–2444
  33. Mamane, Y., Petroulakis, E., LeBacquer, O., and Sonenberg, N. (2006) mTOR, translation initiation and cancer. *Oncogene* **25**, 6416–6422
  34. Sarbassov, D. D., Ali, S. M., and Sabatini, D. M. (2005) Growing roles for the mTOR pathway. *Curr. Opin. Cell Biol.* **17**, 596–603
  35. Ashburner, M., Ball, C. A., Blake, J. A., Botstein, D., Butler, H., Cherry, J. M., Davis, A. P., Dolinski, K., Dwight, S. S., Eppig, J. T., Harris, M. A., Hill, D. P., Issel-Tarver, L., Kasarskis, A., Lewis, S., Matese, J. C., Richardson, J. E., Ringwald, M., Rubin, G. M., and Sherlock, G. (2000) Gene ontology: tool for the unification of biology. The Gene Ontology Consortium. *Nat. Genet.* **25**, 25–29
  36. Mogk, A., Schmidt, R., and Bukau, B. (2007) The N-end rule pathway for regulated proteolysis: prokaryotic and eukaryotic strategies. *Trends Cell Biol.* **17**, 165–172
  37. Seglen, P. O., and Gordon, P. B. (1982) 3-Methyladenine: specific inhibitor of autophagic/lysosomal protein degradation in isolated rat hepatocytes. *Proc. Natl. Acad. Sci. U. S. A.* **79**, 1889–1892
  38. Petiot, A., Ogier-Denis, E., Blommaert, E. F., Meijer, A. J., and Codogno, P. (2000) Distinct classes of phosphatidylinositol 3'-kinases are involved in signaling pathways that control macroautophagy in HT-29 cells. *J. Biol. Chem.* **275**, 992–998
  39. Cuervo, A. M., Palmer, A., Rivett, A. J., and Knecht, E. (1995) Degradation of proteasomes by lysosomes in rat liver. *Eur. J. Biochem.* **227**, 792–800
  40. Cuervo, A. M. (2004) Autophagy: many paths to the same end. *Mol. Cell. Biochem.* **263**, 55–72
  41. Kopitz, J., Kisen, G. O., Gordon, P. B., Bohley, P., and Seglen, P. O. (1990) Nonselective autophagy of cytosolic enzymes by isolated rat hepatocytes. *J. Cell Biol.* **111**, 941–953
  42. Kitagawa, T., and Ono, K. (1986) Ultrastructure of pancreatic exocrine cells of the rat during starvation. *Histol. Histopathol.* **1**, 49–57
  43. Onodera, J., and Ohsumi, Y. (2004) Ald6p is a preferred target for autophagy in yeast, *Saccharomyces cerevisiae*. *J. Biol. Chem.* **279**, 16071–16076
  44. Dengjel, J., Akimov, V., Olsen, J. V., Bunkenborg, J., Mann, M., Blagoev, B., and Andersen, J. S. (2007) Quantitative proteomic assessment of very early cellular signaling events. *Nat. Biotechnol.* **25**, 566–568
  45. Hoyer-Hansen, M., and Jaattela, M. (2008) Autophagy—an emerging target for cancer therapy. *Autophagy* **4**, 574–580
  46. Vabulas, R. M., and Hartl, F. U. (2005) Protein synthesis upon acute nutrient restriction relies on proteasome function. *Science* **310**, 1960–1963